

Electrochemical Behavior of Titanium in NaF Solutions and Characterization of Oxide Film Formed on its Surface

Awad Sadek Mogoda^{1,*} and K. M. Zohdy²

¹ Chemistry Department, Faculty of Science, Cairo University, Giza 12613, Egypt

² Higher Technology Institute, Tenth of Ramadan City, Egypt

*E-mail: awad_mogoda@hotmail.com

Received: 25 February 2020 / Accepted: 1 May 2020 / Published: 10 July 2020

Open-circuit potential, potentiodynamic polarization, cyclic voltammetry and electrochemical impedance spectroscopy (EIS) techniques have been used for studying the corrosion of titanium in sodium fluoride solutions of various concentrations (10^{-3} to 1.5 M). The potential results showed that the native film on titanium surface grows at a rate decreases as F^{-} ion concentration increases. An active-passive transition peak was clearly observed in the voltammetric curves for fluoride concentrations ranging from 10^{-3} to 0.25 M and did no longer appear for concentrations more than 0.25 M due to such high concentrations help in formation of anodic oxide on titanium. The EIS and potentiodynamic polarization results gave more evidence for lowering the protectiveness of the primary passive layer on titanium with increasing fluoride concentration. Scanning electron microscopy (SEM) micrographs conformed the repairing of the cracks and defects present at the primary formed film on titanium surface after immersion in 0.01 M sodium fluoride. Energy dispersive spectroscopy (EDS) spectra found out the presence of titanium oxide layer on the metal surface dipped in fluoride medium. The anodic film on titanium dissolves in fluoride solution because it has greater defective character than the native film which grows in the same solution.

Keywords. Titanium; open circuit potential; cyclic voltammetry; Impedance; SEM; EDS.

1. INTRODUCTION

The high strength to weight ratio of titanium metal and its alloys and their extraordinary corrosion resistance cause them beneficial candidate materials in lots of industrial applications, such as aircraft turbine engine component, aerospace fasteners, automotive, power generation equipments, aeronautic and naval. Titanium and a number of its alloys are extensively used as medical or dental implants in consequence of their good biocompatibility, excellent corrosion resistance, and appropriate mechanical properties [1]. Titanium and most of its alloys are characterized by a high corrosion resistance due to formation of a protecting passive film of TiO_2 [2, 3]. The corrosion behavior for titanium was studied in

HCl, H₂SO₄ and H₃PO₄ [4, 5], and for Ti-6Al-4V alloy in H₃PO₄ [6, 7]. The electrochemical properties of titanium and Ti-6Al-4V alloy were tested in concentrated hydrochloric and sulphuric acids [8], in HCl and H₂SO₄ containing molybdate, metavanadate and iodate anions [9], in hydrobromic acid [10], in azide and halide solutions [11] and in phosphoric acid [12]. It was found that Ti has an excessive tendency to form passive oxide layer in bromide more than in azide and other halide solutions, where the simultaneous increase of the open circuit potential and the oxide film resistance follow the order: Br⁻ > N³⁻ > Cl⁻ > I⁻ > F⁻.

The aim of the existing work is to research the corrosion of titanium and its anodic film stability in distinct concentrations of NaF solutions. In this appreciate, open circuit potential, cyclic voltammetry, potentiodynamic polarization and electrochemical impedance spectroscopy (EIS) techniques were used. The electrochemical measurements have been confirmed via out scanning electron microscopy (SEM) and energy-dispersive X-ray spectroscopy (EDS) spectra.

2. EXPERIMENTAL

2.1. Sample and solution

Pure titanium (99.7 %) was cut as sheets and mounted into glass tubes of appropriate internal diameter with epoxy resin. The exposed surface area of the investigated material was 1.0 cm². The specimen was supplied in the form of foil 0.89 mm thick from Johnson and Mathey (England). Prior to immersion in the electrolyte, the electrodes were abraded using successively grades emery papers down to 2000 grit, then rubbed with a soft cloth until they acquired a mirror-bright surface and rinsed with distilled water. Sodium fluoride solutions of various concentrations (0.001 to 1.5 M) were prepared using Analar grade reagents (BDH) with triple distilled water and adjusted to pH 6.2 [11]. Lactic was used for adjustment the solution pH. The measurements have been achieved in stagnant solutions at 25 °C.

2.2. Electrochemical tests

The open circuit potential, cyclic voltammetry, EIS and polarization (potentiostatic or galvanostatic) measurements were conducted using the electrochemical workstation 1M6e zahner elektrik (GmbH, Meßtechnik, Kronach, Germany) [13, 14]. The Echem Analyst software (version 5.21) was used for all electrochemical data analysis. The electrolytic cell was an all glass double jacket three electrode cell. A platinum metal was used as an auxiliary electrode. All potential were measured and reported against saturated Ag/AgCl electrode as a reference electrode. The EIS measurements were performed at open circuit potential. The input signal was usually 10 mV peak to peak in the frequency range from 0.01 Hz to 10⁵ Hz. Cyclic voltammograms of titanium in sodium fluoride solutions were recorded from -2.25 to 5.00 V at a scan rate of 50 mV s⁻¹. Potentiodynamic scans were traced from -1.5 to 2.0 V vs. Ag/AgCl at a rate of 1 mV s⁻¹. An anodic film was formed galvanostatically on the mechanically polished titanium surface at a current density of 10⁻³ A cm⁻² in naturally aerated 0.05 M sodium fluoride solution.

2.3. Characterization of surface morphologies and composition

The surface morphologies of titanium electrodes were observed by scanning electron microscopy (SEM, Quanta 250 FEG, FEI company, Netherlands). The chemical analysis of titanium surface was performed by energy dispersive X-ray spectroscopy (EDS, X Flash detector 4010, Bruker, Germany).

3. RESULTS AND DISCUSSION

3.1. Effect of NaF concentration

3.1.1. Open circuit potential

The open-circuit potential of the mechanically polished titanium electrode was recorded with time in sodium fluoride solutions of various concentrations (0.001 to 1.5 M) till a steady potential value is reached. The results are represented in Figure 1. It is clear from this Figure that the potential increases gradually with time to more positive value at a rate decreases with increasing fluoride concentration and reaches a steady value after different immersion times in the test solutions depending on their concentrations.

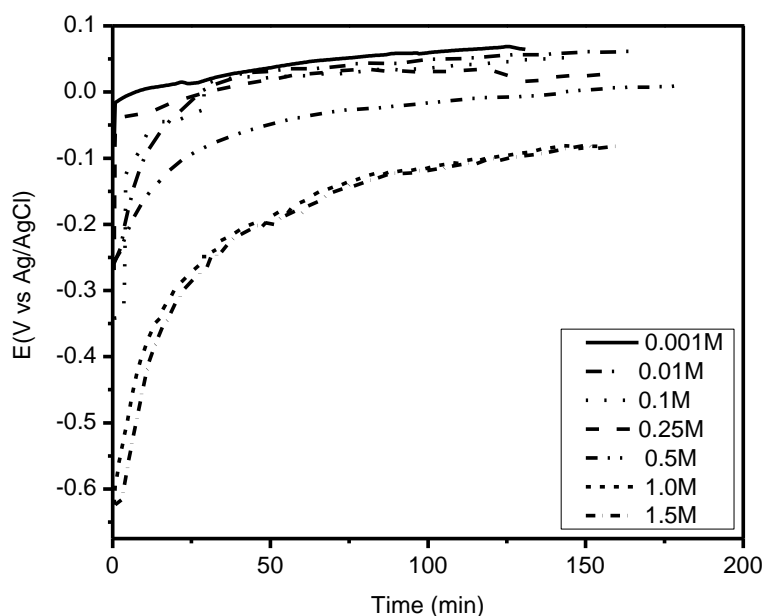


Figure 1. Variation of the open-circuit potential, E, of the mechanically polished Ti surface with time in different NaF concentrations.

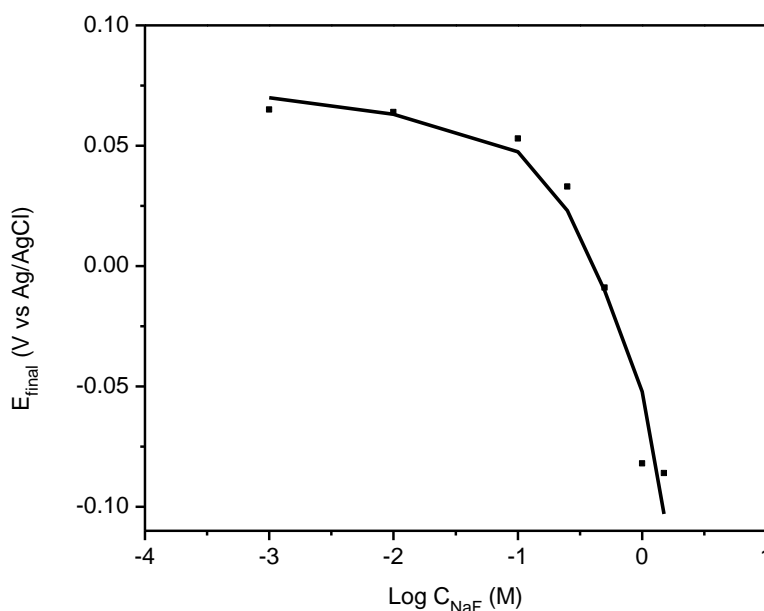


Figure 2. Variation of the steady state potential with NaF concentration.

This indicates that the pre-immersion (air-formed) film on Ti surface increases in thickness with time. Increasing of the open-circuit potential to positive value was observed for Ti in azide and halide anions [11], in H_3PO_4 [12], in HBr [15] and in saliva containing fluoride ions [16]. The final steady potentials values are attained after a time which increases with the increase of F^- ions concentration. Also, the steady state potentials values are shifted to less noble values as NaF concentration increases as shown in Figure 2. Previously, similar observations had been recorded for titanium [17] and niobium [18] in HCl solutions.

Fluoride ions penetrate the formed oxide film through pores and defects, and increase its permeability. Further, the adsorption of fluoride ions on the titanium surface are in competition with the dissolved O_2 or OH^- and this decreases the formation rate of the oxide film on Ti surface [19]. This behavior causes the slowness of the electrode potential in attaining the steady state value as fluoride ions concentration increase.

3.1.2. Cyclic voltammetry

Cyclic voltammograms of Ti electrode were recorded from -2.25 to 5.00 V in various concentrations of NaF solutions (0.001 to 1.5 M) using a scan rate equal to 50 mV s^{-1} as shown in Figure 3.

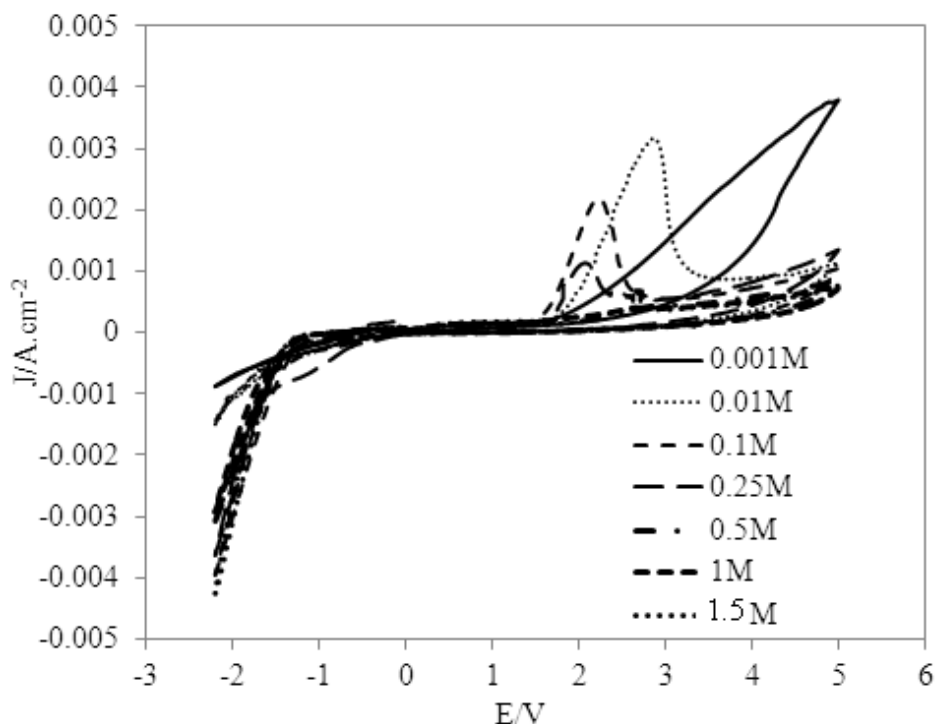


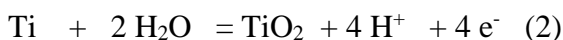
Figure 3. Cyclic voltammograms of Ti in different NaF concentrations at 50 mV/s.

In this Figure, the voltammetric curve of Ti in 0.001 M fluoride solution displays a region of practically constant current which corresponds to growth of a passive film on Ti surface [20] after which the current starts to increase quickly main to a trans-passive region. For fluoride concentrations greater than 0.001 M the voltammetric curves of Ti show a region of constant current and an active – passive transition peak (anodic current peak), which is dwindled with increasing F⁻ ions concentration, and eventually a small passive region.

Through the active region of the anodic current peak (the ascending branch includes an increase of the current) dissolution of titanium proceeds by the anodic process:



The formation of Ti³⁺ was confirmed analytically using spectrophotometric method [21]. Ti³⁺ ions diffuse through the pores of the passive film from the metal substrate to the electrolyte. The presence of oxygen in the electrolyte oxidize Ti³⁺ into Ti⁴⁺. Through the passive region of the anodic current peak (the descending branch comprises decrease of the anodic current) the metal dissolution is hindered and Ti⁴⁺ ions precipitate as TiO₂ on titanium. After this, growth of TiO₂ on titanium occurs according the reaction:



In the reverse potential scan the current decays steadily to zero value without any peak appears within the curve of cyclic voltammogram which well-known shows that the oxide layer formed during the positive scan can not be cathodically reduced. Figure 4 shows SEM micrograph of the titanium surface after one entire potential scan in 0.5 M NaF solution at 50 mV/s which reveals the growth of the anodic oxide on the metal surface.



Figure 4. SEM micrograph of the titanium surface after one entire potential scan in 0.5 M NaF solution at 50 mV/s.

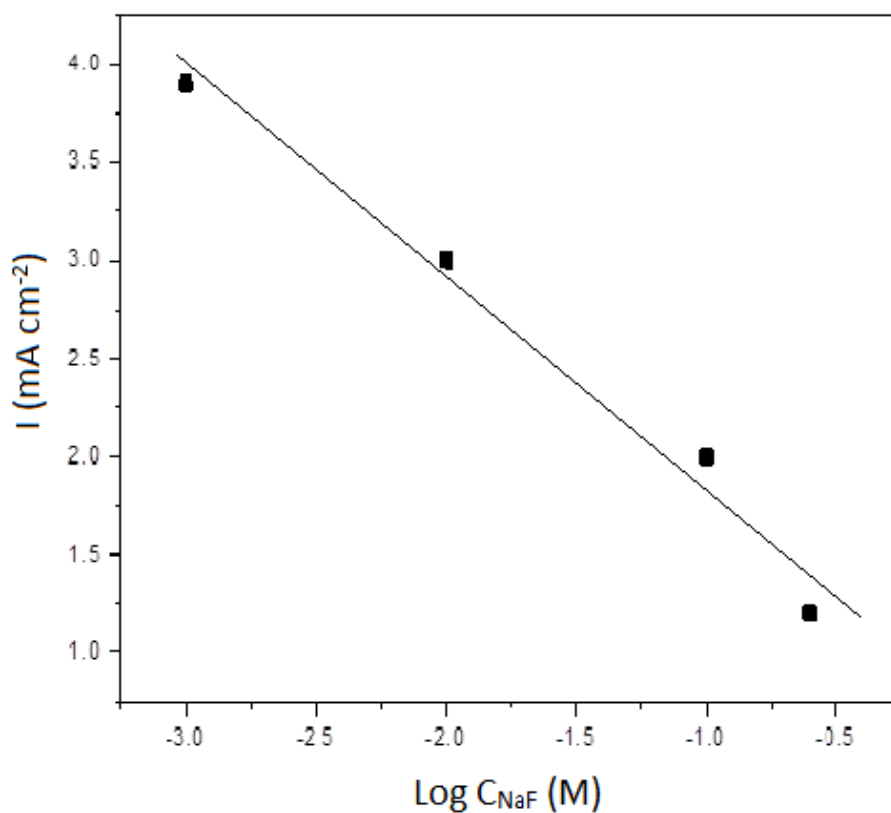


Figure 5. Dependence of the maximum current density of the anodic current peak on NaF concentration.

The variation of maximum current density of the anodic current peak with NaF concentration is given in Figure 5, which demonstrates that the metal dissolution is inhibited as fluoride ions

concentration increases. For F^- ions concentrations more than 0.25 M, the height of the anodic peak seems as extremely small which means that most of titanium oxide was formed by reaction (2). This means that fluoride concentrations more than 0.25 M assist effectively in continuous growth of the oxide on titanium greater than the lower concentrations. This may be due to the adsorption of F^- ions at high concentration on the anodic titanium surface retards its dissolution.

3.1.3. EIS studies

The EIS spectra have been recorded for titanium electrode in NaF solutions of different concentrations (0.001 to 1.5 M) at open-circuit potential. The results are shown as Nyquist plots in Figure 6. These outcomes reveal that the capacitive semicircle decreases in size with increasing fluoride ions concentration. This means that the resistance of Ti surface for corrosion decreases as F^- ions concentration increases, similar results were observed for titanium in saliva containing fluoride [22, 23].

Figure 7 represents the more suitable equivalent electrical circuit for fitting the impedance spectra for titanium in fluoride solutions. Studies done before on Ti showed that this electrical circuit may be used effectively for fitting the experimental results of impedance [11, 12]. The components of this equivalent electrical circuit are as follows: R_s solution resistance; C_{dl} double layer capacitance with constant phase angle element (CPE) behavior; R_{ct} charge transfer resistance that related to the corrosion process; C_f capacitance due to the dielectric nature of the surface film and R_f resistance due to the surface film. Since there is a variance between real capacitance and pure capacitance therefore, computer simulation of the EIS spectra can be carried out by replacing the capacitance C, with a constant phase element (CPE). The impedance of CPE is described by the following expression [24]:

$$Z_{CPE} = [(j\omega)^\alpha Y]^{-1} \quad (3)$$

where Y is the frequency independent real constant of the CPE, ω the angular frequency, $j = \sqrt{-1}$, and α is an adjustable empirical exponent which varies between 1.0 for a perfect smooth surface with pure capacitive behavior and 0.5 for a porous surface.

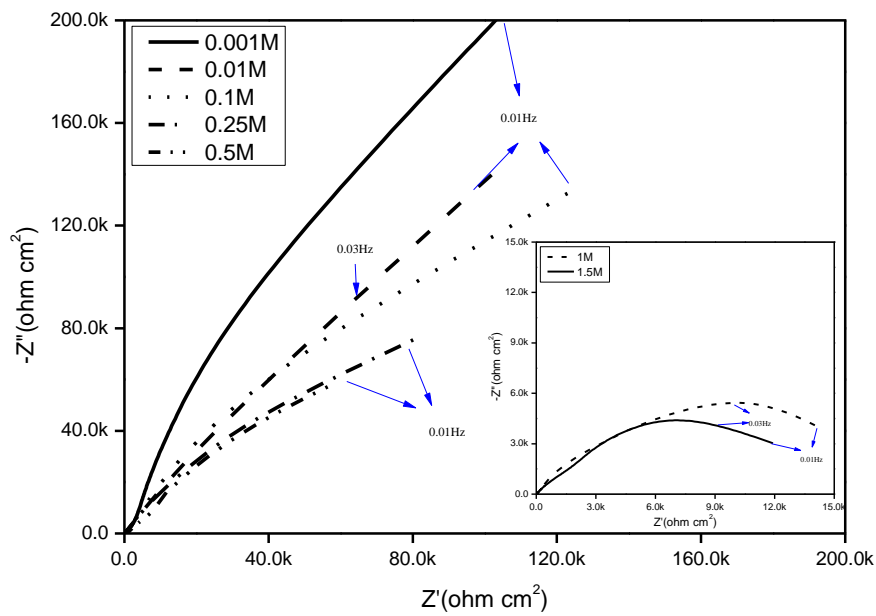


Figure 6. Nyquist plots of Ti in different NaF concentrations.

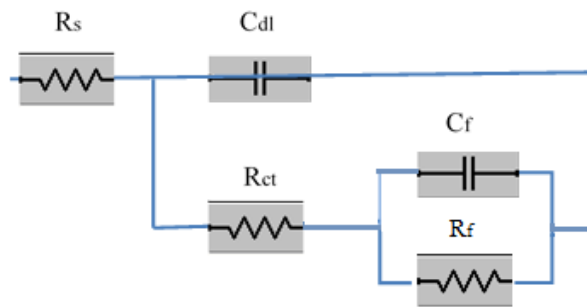


Figure 7. Equivalent electrical circuit model used to fit the EIS experimental results.

Table 1. Characteristic parameters for fitting the experimental EIS results of titanium in different NaF concentrations.

NaF (M)	R _f (kΩ cm ²)	C _f (μF cm ⁻²)	α	R _{ct} (kΩ cm ²)	C _{dl} (μF cm ⁻²)	R _s (Ω)
0.001	490.40	55.89	0.83	11.29	6.07	48
0.01	248.10	85.63	0.84	9.64	7.53	37
0.10	230.41	97.16	0.85	8.99	9.22	33
0.25	133.11	115.90	0.84	7.91	10.35	40
0.50	109.39	128.40	0.83	7.41	11.40	43
1.00	14.17	146.50	0.83	1.31	16.76	47
1.50	10.94	163.20	0.82	1.27	21.11	38

The fitted characteristic parameters for Ti in the fluoride solutions are listed in Table 1. In this Table, the experimental values of α are ranged between 0.82 and 0.85 which indicate that the passive oxide film of titanium does not behave as perfect capacitor. Also we note from Table 1 that the resistance, R_f , of the primary formed film on titanium decreases and consequently its capacitance, C_f , increases as fluoride concentration increases indicating the decreasing of the protectiveness of such film.

3.1.4. Potentiodynamic polarization curves analysis

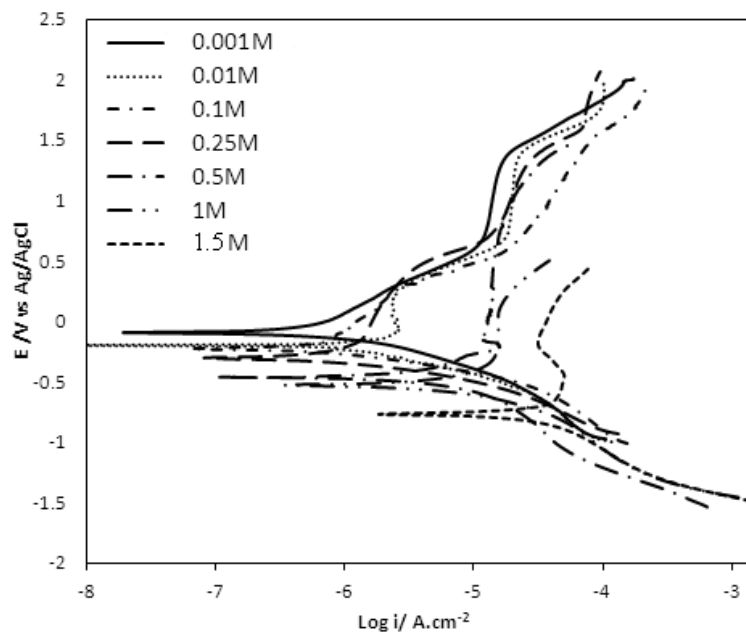


Figure 8. Potentiodynamic polarization curves of Ti in different NaF concentrations.

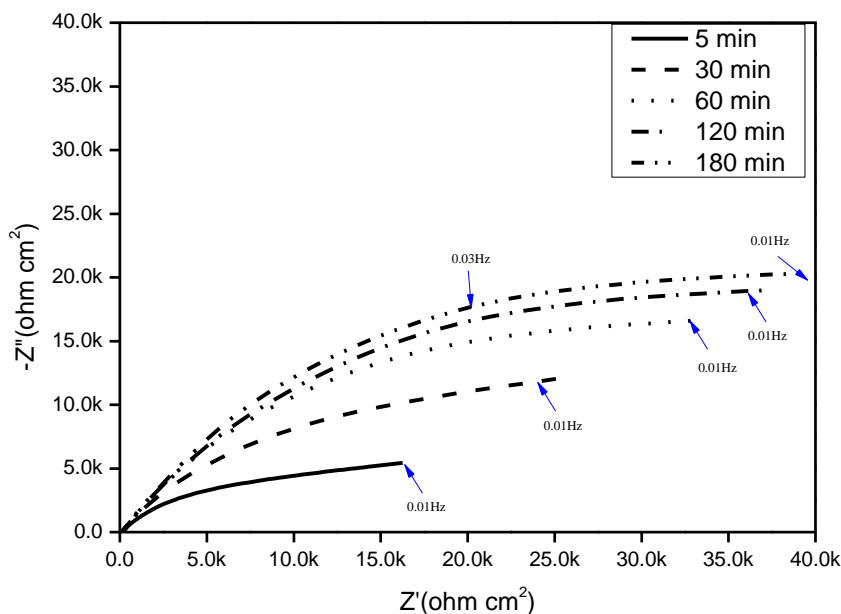
Table 2. Potentiodynamic polarization results of titanium in different NaF concentrations.

NaF Concentration (M)	E_{corr} mV	I_{corr} $\mu\text{A}/\text{cm}^2$	Corrosion rate mpy
0.001	-95	0.39	0.60
0.01	-199	1.14	2.05
0.10	-248	1.34	2.09
0.25	-226	1.44	2.25
0.50	-306	1.63	2.55
1.00	-224	1.81	2.83
1.50	-755	11.90	18.57

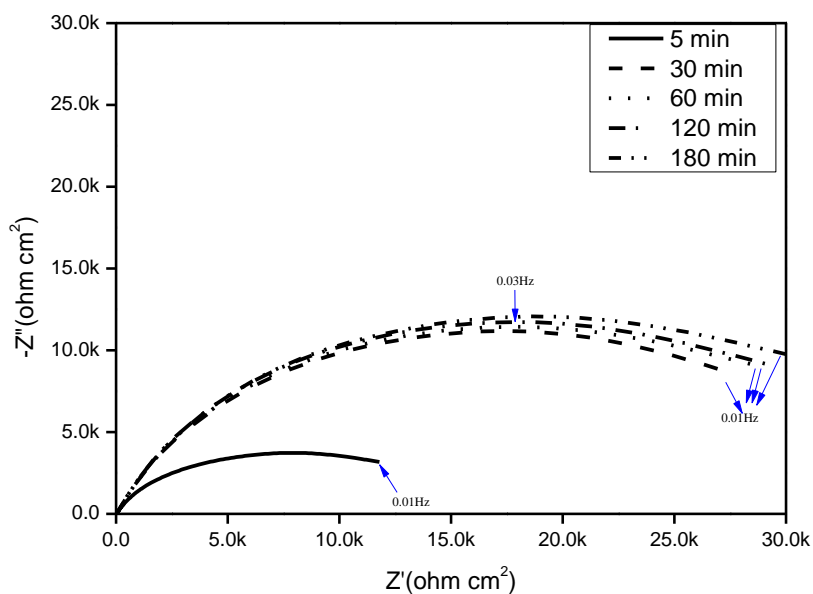
Figure 8 shows the potentiodynamic polarization curves of Ti in various NaF concentrations. The corrosion current, I_{corr} , corrosion potential, E_{corr} , and corrosion rate in mpy of Ti in fluoride solutions are presented in Table 2.

It is obvious from the polarization data that as the F- ions concentration increases the corrosion rate of titanium also increases, that is inconsistent with the results of EIS.

3.2. Effect of immersion time



A



B

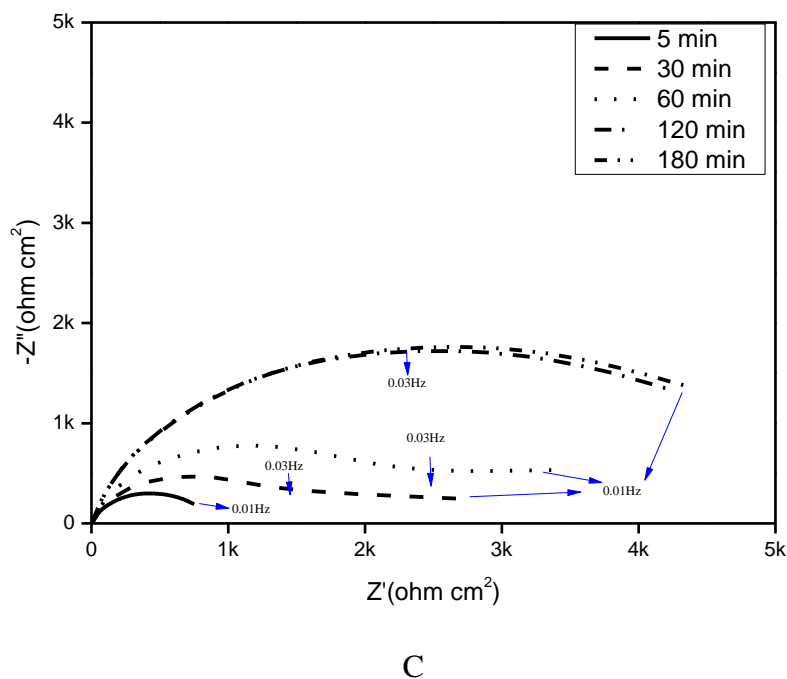
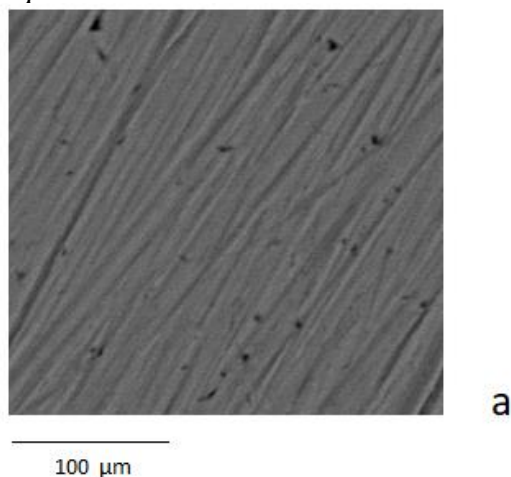


Figure 9. Nyquist plots of Ti at different times in (a) 0.01 M NaF, (b) 1.0 M NaF and (c) 1.5 M NaF.

EIS spectra of titanium electrode had been measured over different periods of immersion time: 5, 30, 60, 120 and 180 min in NaF of different concentrations: 0.01, 1.0 and 1.5 M and the results are given in Figure 9a-c. In this Figure, the diameter of the capacitive semicircle increases with increasing the immersion time in the three test solutions indicating growth of the native film on the titanium metal. Also, the impedance value at any defined time decreases as F^- ions concentration increases for example after immersion time of 180 min the impedance is highest in 0.01 M salt solution and is lowest in 1.5 M and intermediate in 1.0 M. This due to the aggressiveness nature of fluoride ions and the effects in Figure 9 are regular with the ones in Figure 6. Recently, we observed that the native film on bismuth surface grows in hydrochloric acid solution as time passes [25].

3.3. Surface morphology and composition



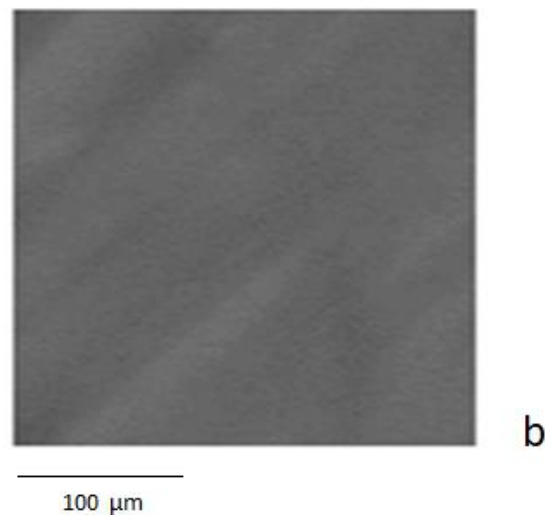


Figure 10. SEM micrographs of the mechanically polished titanium surface before (a) and after (b) immersion in 0.01 M NaF solution for 180 min.

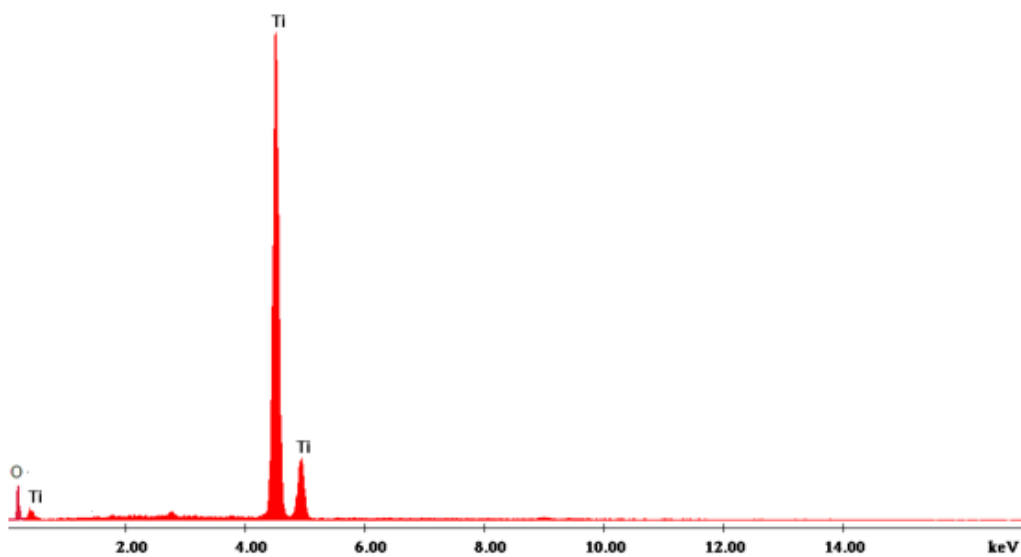


Figure 11. EDS spectra of titanium surface after immersion in 0.01 M NaF solution for 180 min.

The morphology and composition of the protective film formed on titanium surface in 0.01 M NaF solution have been studied through scanning electron microscopy and EDS, respectively. Figure 10a and b shows the SEM micrographs of the mechanically polished titanium surface before and after immersion in 0.01 M NaF solution for 180 min. It is clear that the scratches and notches which seem in the air-formed film on titanium surface in Figure 10a were reduced because of growth of this film in sodium fluoride as proven in Figure 10b. The EDS spectra in Figure 11 conform that the film grew on titanium surface in fluoride solution consists of titanium oxide.

3.4. Stability of anodic film on titanium in NaF

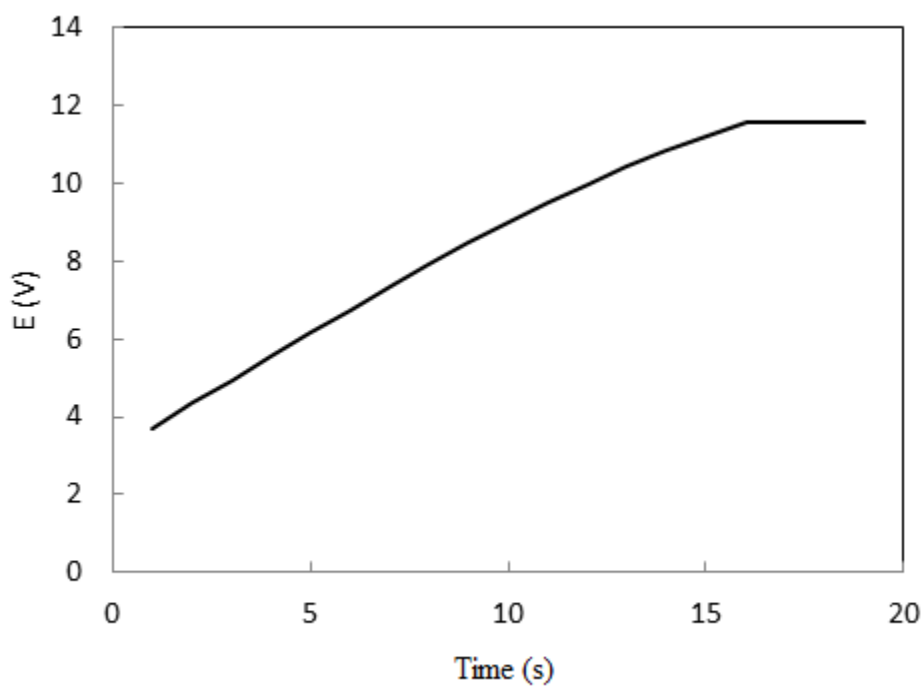


Figure 12. Change of the anodic potential of titanium with time in 0.05 M NaF.

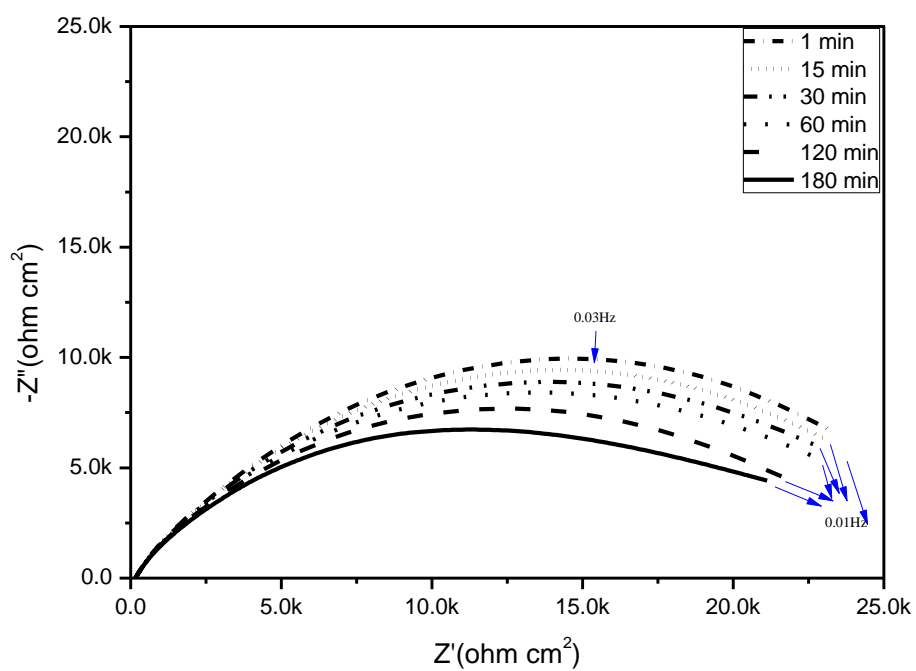


Figure 13. Nyquist plots for anodic film on Ti at different intervals of time in 0.1 M NaF.

Formation of an anodic film was conducted galvanostatically on the mechanically polished titanium surface at a current density of $10^{-3} \text{ A cm}^{-2}$ in naturally aerated 0.05 M sodium fluoride solution. The variation of the anodic potential of titanium electrode with time in 0.05 M sodium fluoride solution is shown in Figure 12. As may be visible from this Figure, the anodic potential rises linearly with time, reaches a maximum value (approximately 12 V) and thereafter, stays steady. This means that the oxide layer grows at steady rate through the linear increase of potential with time and the deviation of the polarization curve from linearity may be due to the occurrence of changes in the oxide film structure, e.g. crystallization [26]. Evidence for this phenomenon has been presented previously during anodization of antimony in sulphuric acid containing potassium dichromate [27]. The defect character within the oxide film increases during the crystallization causing reactions other than oxide growth such as oxide dissolution and oxygen evolution. Previously, we found that the film made galvanostatically on titanium in 0.1 N H_2SO_4 up to 15 V has a larger thickness than the other films and has high insulating properties in phosphoric acid [28].

After formation of the anodic film on Titanium the current was cut and the electrode was rinsed with distilled water and transferred quickly to 0.1 M NaF solution whereas the EIS was measured at time intervals up to 1, 15, 30, 60, 120 and 180 min. The results in Figure 13 reveal that the semicircle size decreases with increasing the time of dipping of the anodic film on titanium in fluoride solution. Also, from the results in Figure 14 it is clear that the anodic film resistance on titanium, R_f , decreases with increasing of the immersion time. This behavior of the anodic oxide layer may be due to dissolution and thinning of this film which is thicker and has greater defective characters than the air-formed film. The later showed a growth behavior in fluoride solution as indicated from the results in Figure 9.

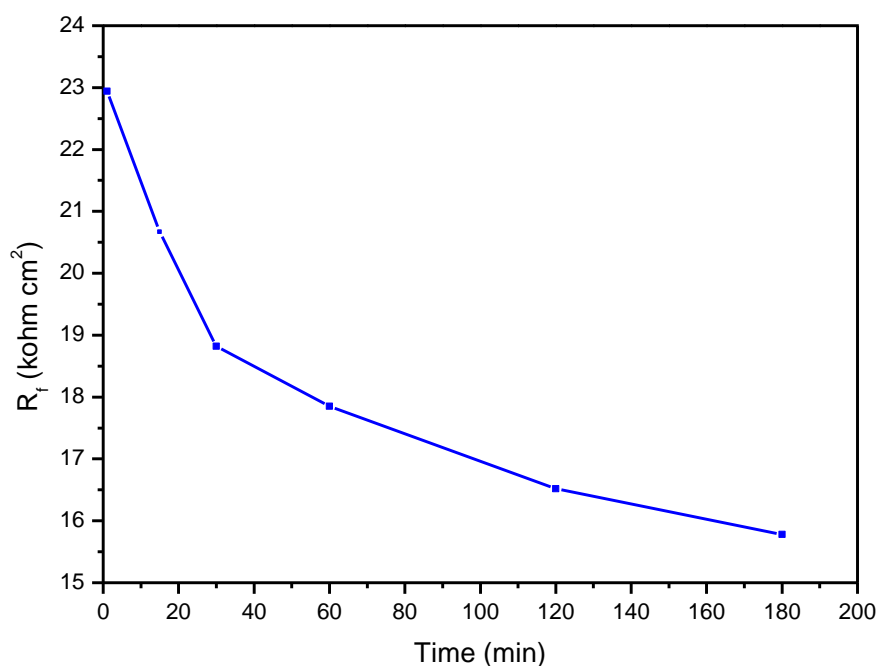


Figure 14. Change of the resistance of the anodic film on titanium, R_f , with time in 0.1 M NaF.

A similar behavior was observed before for the dissolution of the anodic oxide on titanium in H_3PO_4 solutions [28] and on antimony in sodium chloride [29] and sodium fluoride media [30].

4. CONCLUSIONS

Aqueous sodium fluoride solutions of concentrations in the range from 0.001 to 1.5 M are suitable for growth of the native film on titanium surface as revealed from the increasing in both the open-circuit potential and the impedance values as time passes. Cyclic voltammograms of titanium in fluoride solution of concentrations greater than 0.25 M showed extremely small active-passive peak which indicates that the passive film on titanium grows continuously. Corroding of titanium increases with increasing of fluoride ions concentration as revealed from the potentiodynamic polarization results.

SEM photographs conform repairing of the flawed regions on titanium surface due to growth of the passive film on its surface in NaF solution. Oxide film was formed on titanium in the fluoride solution as examined by EDS spectra. The oxide film formed anodically on titanium in 0.05 M NaF is unstable and suffers from dissolution in sodium fluoride solution.

References

1. G.R. Parr, L.K. Gardner and R.W. Toth, *J. Prosthet Dent.*, 54 (1985) 410.
2. K. Elagli, M. Traisnel and H.F. Hidebrand, *Electrochim. Acta*, 38 (1993) 1769.
3. I. Milosev, B. Kapun and V.S. Selih, *Acta Chim. Slov.*, 60 (2013) 543.
4. A. Rauscher and Z. Lukacs, *Werkst. Korros.*, 39 (1988) 280.
5. V.B. Singh and M.A. Hosseini, *Corros. Sci.*, 34 (1993) 1723.
6. V.B. Singh and M.A. Hosseini, *J. Appl. Electrochem.*, 24 (1994) 250.
7. D.D.N. Singh, *J. Electrochem. Soc.*, 132 (1985) 378.
8. A.S. Mogoda, Y.H. Ahmad and W.A. Badawy, *J. Appl. Electrochem.*, 34 (2004) 873.
9. A.S. Mogoda, Y.H. Ahmad and W.A. Badawy, *Mater. Corrosion*, 55 (2004) 449.
10. A.A. Ghoneim, F. El-Taib Heakal, A.S. Mogoda and Kh.A. Awad, *Surf. Interface Anal.*, 42 (2010) 1695.
11. F. El-Taib Heakal, A.A. Ghoneim, A.S. Mogoda and Kh.A. Awad, *Corros. Sci.*, 53 (2011) 2728.
12. A.A. Ghoneim, A.S. Mogoda, Kh.A. Awad and F. El-Taib Heakal, *Int. J. Electrochem. Sci.*, 7 (2012) 6539.
13. Y. H. Ahmad, A.S. Mogoda and A.G. Gadallah, *Int. J. Electrochem. Sci.*, 7 (2012) 4929.
14. A.S. Mogoda and Y.H. Ahmad, *Silicon*, 11 (2019) 2837.
15. F. El-Taib Heakal and Kh.A. Awad, *Int. J. Electrochem. Sci.*, 6 (2011) 6483.
16. R.H. Tammam, A.S. Mogoda and S.G. Abd El-Kader, *Al Azhar Bull. Sci.*, 29 (2018) 71.
17. M.S. El-Basiouny and A.G. Gadallah, *Ann. Chim.*, 71(1981) 391.
18. M.S. El-Basiouny, A.M. Bekheet and A.G. Gadallah, *Corrosion*, 40 (1984) 116.
19. T.P. Hoar, D. Mears and G. Rothwell, *Corros. Sci.*, 5 (1965) 279.
20. A. Fossati, F. Borgioli, E. Galvanetto and T. Bacci, *Corros. Sci.*, 46 (2004) 917.
21. J. Krysa, R. Mraz and I. Rousar, *Mater. Chem. Phys.*, 48 (1997) 64.
22. A. Robin and J.P. Meirelis, *J. Appl. Electrochem.*, 37 (2007) 511.
23. A. Stájer, K. Ungvári, I.K. Pelsőczy, H. Polyánka, A. Oszkó, E. Mihalik, Z. Rakonczay, M. Radnai, L. Kemény, A. Fazekas and K. Turzó, *J. Biomed. Mater. Res. A*, 87 (2008) 450.
24. K. Juttner, *Electrochim. Acta*, 35 (1990) 1501.

25. A.S. Mogoda, *Bull. Mater. Sci.*, 43 (2020) 100.
26. D.M. Lakhiani and L.L. Shreir, *Nature*, 188 (1960) 49.
27. A.S. Mogoda and T.M. Abd El-Haleem, *Corrosion*, 59 (2003) 3.
28. F. El-Taib Heakal, A.S. Mogoda, A.A. Mazhar and M.S. El-Basiouny, *Corros. Sci.*, 27 (1987) 453.
29. M.M. Hefny, W.A. Badawy, A.S. Mogoda and M.S. El-Basiouny, *Electrochim. Acta*, 30 (1985) 1017.
30. W.A. Badawy, A.S. Mogoda and M.M. Ibrahim, *Electrochim. Acta*, 33 (1988) 1367.

© 2020 The Authors. Published by ESG (www.electrochemsci.org). This article is an open access article distributed under the terms and conditions of the Creative Commons Attribution license (<http://creativecommons.org/licenses/by/4.0/>).